

Simulation of rarefied gas flow and heat transfer in microchannels

WANG Xian (王 嫻)¹, WANG Qiuwang (王秋旺)¹,
TAO Wenquan (陶文铨)¹ & ZHENG Ping (郑 平)²

1. School of Energy & Power Engineering, Xi'an Jiaotong University, Xi'an 710049, China;

2. Department of Mechanical Engineering, Hong Kong University of Science and Technology, Hong Kong, China

Correspondence should be addressed to Wang Qiuwang (email: wangqw@xjtu.edu.cn)

Received June 18, 2001

Abstract Analysis and simulation of rarefied nitrogen gas flow and heat transfer were performed with the Knudsen number ranging from 0.05 to 1.0, using the direct simulation of Monte Carlo (DSMC) method. The influences of the Kn number and the aspect ratio on the gas temperature and wall heat flux in the microchannels were studied parametrically. The total and local heat fluxes of the microchannel walls varying with the channel inlet velocities were also investigated in detail. It was found that the Kn number and the aspect ratio greatly influence the heat transfer performance of microchannels, and both the channel inlet and outlet have higher heat fluxes while the heat flux in the middle part of channels is very low. It is also found that the inlet free stream flow velocity has small affect on the wall total heat flux while it changes the distribution of local heat flux.

Keywords: microchannel, Kn number, DSMC, fluid flow and heat transfer.

Fluid flow and heat transfer can be studied at either macroscopic or microcosmic levels. The rapid development of MEMS has enabled us to investigate the fluid flow and heat transfer in micro-dimensional devices^[1]. However, the Navier-Stokes equation used for continuum flow is often not suitable for the fluid flow described by Boltzmann equation in micro-dimensional device. The gas flow can be divided into four domains^[2] based on the Kn number which gives the rarity of the gases. It is defined as

$$Kn = \lambda/L, \quad (1)$$

where λ is the gas mean free path; L is the characteristic length. Generally, the Navier-Stokes equation loses its validity when $Kn > 0.1$, so the gas macroscopic properties should be obtained by the statistical method at the microcosmic level. But based on the current knowledge, it is very hard to obtain the analytical solution of Boltzmann equation. For these reasons, to satisfy the needs for numerical simulations of rarefied gas, Bird et al. proposed a new method to simulate gas flow and heat transfer in the 1960s—direct simulation of Monte Carlo (DSMC) method^[3]. It proves a powerful tool to solve such problems when $Kn > 0.1$.

In this paper, with the aid of DSMC method, the analysis and investigation were made carefully aiming at the subsonic flow in a microchannel with the Kn number ranging from 0.05 to 1.0. In order to investigate the influence factors on the heat transfer performance in microchannels, a few cases with different aspect ratios were simulated and compared for every Kn number.

1 Numerical methods

DSMC method was derived from molecular gas dynamics; it does not solve the Boltzmann equation directly, but imitates the real physical process described by this equation. In DSMC method, the real gas was modeled by a large number of simulated molecules. This probabilistic procedure depends on the dilute gas assumption. The essential DSMC approximation is the uncoupling, over a small time interval, of the molecular motion and intermolecular collisions, so we can follow the trajectories of the very large number of simulated molecules simultaneously using a computer and record their microcosmic properties. Then the macroscopic properties may be identified with average values of the appropriate molecular quantities at any location in the flow. The molecule movement routines are trivial, and a simple indexing of the molecules to sub-cells and cells causes all collisions to be between near neighbors. The procedures for the establishment of the correct collision rate are based on the cells, while individual collision pairs. In order to make the typical simulated molecules remain in a cell at least one time step, the cell's dimension is of the order of the local mean free path. On the other hand, to implement the uncoupling of molecular movement and collision, the time step should be smaller than the mean collision time.

Nitrogen was used as the working fluid in this work. Because of the differences among the structures of monatomic, diatomic and polyatomic molecules, the solving methods involved in the DSMC procedure are also different. Monatomic molecules only have translational energy, so the intermolecular collision should be regarded as elastic. However, diatomic and polyatomic molecules also include rotational and vibrational energy, hence the collisions are inelastic. But the molecular characteristic temperature related to vibration is so high (for example, the temperature for nitrogen is 3337 K) that the temperatures of most working conditions are not high enough to excite the vibrational mode. So in the common cases, it is reasonable not considering vibration energy in simulation^[5]. If a collision is regarded as inelastic, although the total energy does not change, it may be reassigned between the translational and internal modes. Whether the total energy is reassigned or not depends on the rotational and vibrational relaxation collision numbers, Z_{rot} and Z_{vib} , which are functions of the temperature. A general Larsen-Borgnakke distribution^[3] function for division of energy between the translational and internal modes was adopted in this paper and the overall kinetic gas temperature may be defined as the weighted mean of the translational and internal temperature based on the degrees of freedom,

$$T = \frac{3T_{tr} + \zeta_{rot}T_{rot} + \zeta_{vib}T_{vib}}{3 + \zeta_{rot} + \zeta_{vib}}, \quad (2)$$

where 3 is the number of translational degree of freedom. For DSMC method, in spite of the space dimension, the velocity must be treated as three-dimensional; ζ_{rot} and ζ_{vib} stand for the number of rotational and vibrational degrees of freedom respectively; T_{tr} , T_{rot} and T_{vib} stand for the temperatures related to translation, rotation and vibration, respectively.

The heat flux through a surface is also the result of molecule-surface interaction which can be defined as

$$q_w = \frac{\sum E_i - \sum E_r}{\Delta t \cdot A}, \quad (3)$$

where the subscripts i and r refer to the incident and reflect molecules respectively, E is the total energy, including translational and internal energy, m is the molecule mass, while Δt and A

represent time and area.

The temperature of the reflected molecules can be adjusted by the thermal accommodation coefficient:

$$\alpha_c = \frac{q_i - q_r}{q_i - q_w}, \quad (4)$$

where q_i and q_r are the incident and reflected energy fluxes, while q_w is the energy flux carried away by the reflected molecules when $T_r = T_w$. It is obvious that α_c ranges from 0 to 1.

2 Physical problem and simulation results

2.1 Physical problem

The microchannel model is shown in fig. 1. The gas in the channel is nitrogen; a free stream at atmosphere with a temperature of 273K and velocity of 100 m/s flows into the microchannel. The temperature of the two wall surfaces of the microchannel was kept at 500 K. Computations were conducted for five Kn numbers: 0.05, 0.08, 0.25, 0.75, and 1.0. For each of them, comparison was made among three aspect ratios, that is, $AR = 5, 15, 25$.

The time step was 10^{-11} s and the stream boundary condition was used at the inlet and outlet. Variable hard sphere (VHS) model was adopted as the molecular model^[3]. For the surface boundary, diffuse reflection model was used, in which the velocity of each molecule after reflection is independent of its incident velocity. The velocities of the reflected molecules as a whole are distributed in accordance with the Maxwellian distribution^[3]:

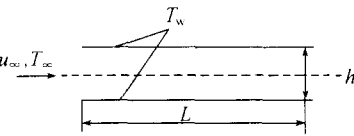


Fig. 1. Microchannel sketch.

$$f(c') = \left(\frac{m}{2\pi\kappa T_r} \right)^{\frac{3}{2}} \cdot e^{-\frac{mc'^2}{2\kappa T_r}}, \quad (5)$$

where c' is the molecule thermal velocity, m is the molecule mass, κ is the Boltzmann constant and T_r is the temperature of reflected molecule. In this paper, the thermal accommodation coefficient α_c was taken to be unity; that is, $T_r = T_w$.

In addition, the number of the simulated molecule must be reasonable for both computational efficiency and physical reliability. If the number is too small, the results will lose their statistic meanings and if it is too large, the computational time would increase greatly. According to Bird^[6], there must be 20—30 simulated molecules in a cell. During the simulation, the numbers of the simulated molecules in cells are usually not constant, but change slightly in the subsonic flow. Therefore in our work, the same weighted factor (the number of actual molecules represented by one simulated molecule) was chosen in all cells, and the average number of simulated molecules per cell is 25—35.

2.2 Results and analysis

The variation of heat flux through microchannel's surface with the Kn number when $AR = 5$ is shown in fig. 2. By eq. (3), the negative heat flux indicates that heat is transferred from surfaces to gas. Fig. 2 shows that in the range of $Kn = 0—10$, which includes the whole transitional region, the surface heat flux increases with an increase in Kn number. When $Kn < 1$, the heat flux increases rapidly and when $Kn > 1$ the increase slows down. This is mainly because of the fact that the higher the Kn number, the more rarefied the gas. So with an increase in Kn number the molecule-surface collision frequency becomes much higher, while the collision of intermolecu-

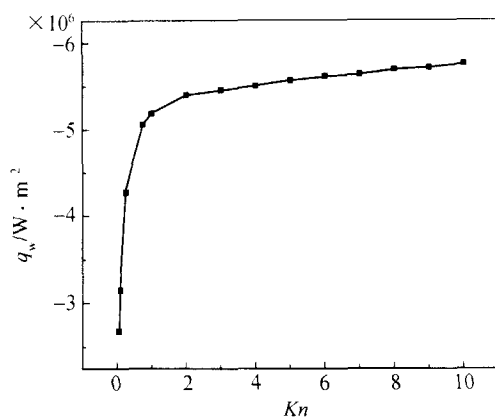


Fig. 2. Variation of heat flux with the Kn number when $AR = 5$

certain degree, although the intermolecular collision decreases, the number of molecules colliding with surface does not increase appreciably, resulting in only a moderate increase in the surface heat flux in the high Kn number region.

Fig. 3 shows the variation of local heat flux in the flow direction under different Kn number when $AR = 5$, and fig. 4 shows the gas temperature variation accordingly. From these two figures, it can be found that the varying trend of heat flux is almost the same for different Kn numbers: the heat fluxes at inlet and outlet are much higher than those at the middle part of the channels. This phenomenon was also reported by Mavriplis et al.⁷¹

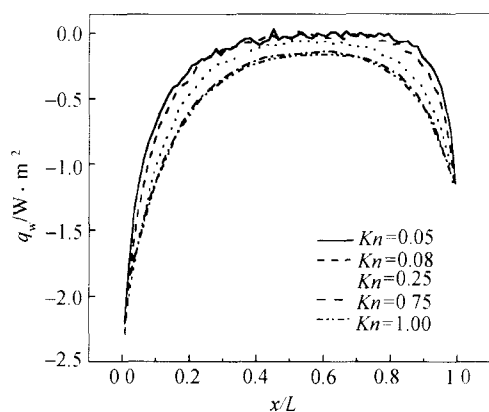


Fig. 3. Variations of local heat flux in the flow direction at different Kn numbers with $AR = 5$.

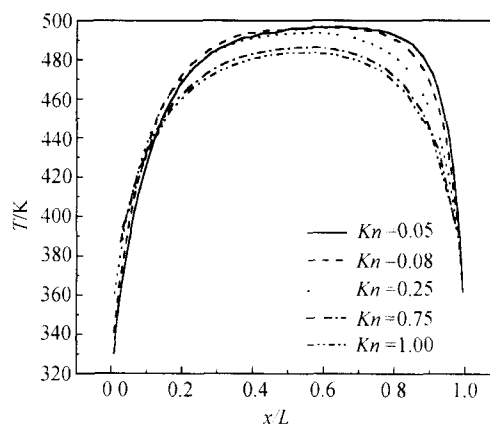


Fig. 4. Variations of local temperature in the flow direction at different Kn numbers with $AR = 5$.

Figs. 5 and 6 show the variations of local heat flux and gas temperature in the flow direction at different AR when $Kn = 0.25$. Fig. 5 indicates that the higher the AR is, the lower the local heat flux will be. While with the decrease in the aspect ratio, the heat flux in the middle part increases. When AR is increased, the gas entering the microchannel is heated rapidly, the heat fluxes increase in the inlet and outlet but are close to zero in the middle part because the gas temperature is nearer to that of the surface (fig. 6). Most part of the channel keeps almost adiabatic and the flow is almost isothermal. However, the dimensional starting point of the adiabatic region is nearly the same for different AR , in the order of 10^{-7} m.

lar decreases. In the free molecule region ($Kn > 10$), the intermolecular collision frequency can be ignored compared with that between molecule and surface. So in this circumstance, the surface heat flux is mainly dependent on the molecule-surface collision. When the Kn number is low, the intermolecular collision is dominant, especially in continuum flow ($Kn < 10^{-3}$), and only those molecules close to the surface can collide with the surface, resulting in a decrease in the surface heat flux. That is why the surface heat flux of a microchannel (10^6 – 10^7 W/m^2) is much higher than that of the macroscopic channel (usually less than 10^4 W/m^2). When the Kn number increases to a

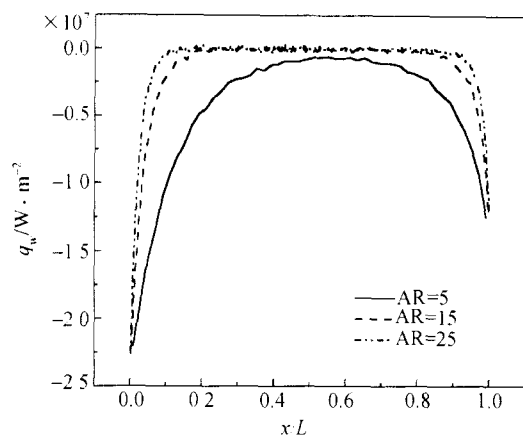


Fig. 5. Variations of local heat flux in the flow direction under different AR with $Kn = 0.25$.

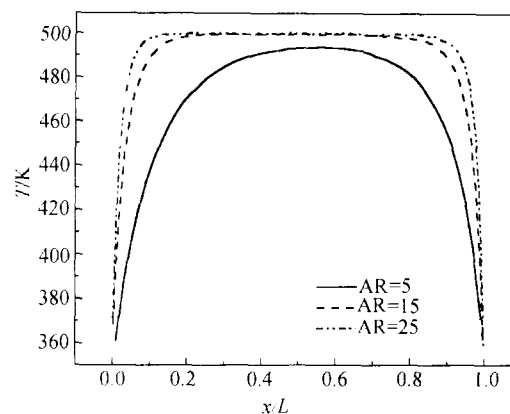


Fig. 6. Variations of local temperature in the flow direction under different AR with $Kn = 0.25$.

The phenomena shown in figs. 3—6 are quite different from the continuum flow. The main reason is that there are molecules entering into and escaping from microchannel both in its inlet and outlet, and the number of which can be obtained by the theory of molecular gas dynamics^[3]. Once the molecules enter into the microchannel, the molecules move arbitrarily with their thermal velocities in every direction with equal opportunity. Therefore, there are molecules escaping from both inlet and outlet of the channel. The energy of entering molecules in the channel inlet and outlet is much different from that of the molecules in the channel. After the gas enters into channel, it becomes much more rarefied, and almost all entering molecules would collide with the surface, so there is a large amount of energy exchange at the channel inlet and outlet. On the other hand, the heat transfer is somewhat enhanced due to the escaping molecules with high energy in the inlet and outlet, which causes a decrease in the mean molecular temperature. The combination of the above two factors (with the first one dominating) results in a rapid increase in the heat flux in inlet and outlet. As long as the free stream velocity is larger than zero, the number of entering molecules in the inlet will be larger than that in the outlet, so the heat flux in inlet is much higher. In the middle part of the channel, although there is a large amount of molecules colliding with the surface, the energy of these molecules is close to that of the surface through colliding frequently with the surface, so that the molecule-surface interaction will exchange very small energy.

For the smaller AR (such as AR = 5 in fig. 6), the gas molecules have not enough chances to collide with the surface before they escape from the channel, which results in large energy difference between the molecules and wall surface; therefore heat exchange will happen all over the channel.

Fig. 7 shows the temperature distribution in the direction perpendicular to the gas flow at the

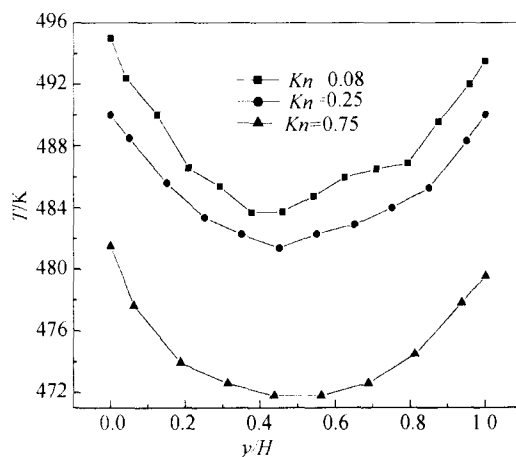


Fig. 7. Temperature distribution in the direction perpendicular to the gas flow at the cross section $x/L = 0.3$ with AR = 5.

cross section $x/L = 0.3$ when $AR = 5$. It can be seen that on the surface ($y/H = 0.0$ and 1.0), there exists a temperature slip region (that is, the temperatures for $y/H = 0.0$ and 1.0 are not equal to the given wall temperature, 500 K). With the increase in Kn number, the slipping temperature difference increases.

Figs. 8 and 9 represent the variations in the total and local heat flux with subsonic stream velocity u_∞ , with $Kn = 1.0$ and $AR = 5$. Here the analysis is only focused on the cases with small AR . Fig. 8 shows that the total heat flux varies with u_∞ very slightly, but the distribution of local heat flux is changed by u_∞ (fig. 9). When u_∞ is lower, the heat flux in the inlet and outlet is almost the same. With the increasing u_∞ , the heat flux increases in the inlet and decreases in the outlet but in the middle part, the heat flux hardly changes with u_∞ . This is because when u_∞ increases, the number of entering molecules in the inlet will increase and those in the outlet will decrease. In our work, the ratios between the entering molecules in inlet and outlet for $u_\infty = 10$ m/s, 100 m/s, 300 m/s are approximately $1:1$, $2:1$, $15:1$ respectively. So the increasing u_∞ enlarges the number of entering molecules, whose energy level is quite different from the surface, and the heat exchange due to the collision increases accordingly. When the outer macroscopic flow velocity is supersonic or even larger, the vacuum boundary condition can be used on the outlet of the channel; that is, there are no molecules entering in the outlet. Under this circumstance, the heat transfer trend in the outlet is almost the same as that in the middle part of the channel, and the heat flux will approach zero. This point of view was also confirmed by Mavriplis et al.^[7].

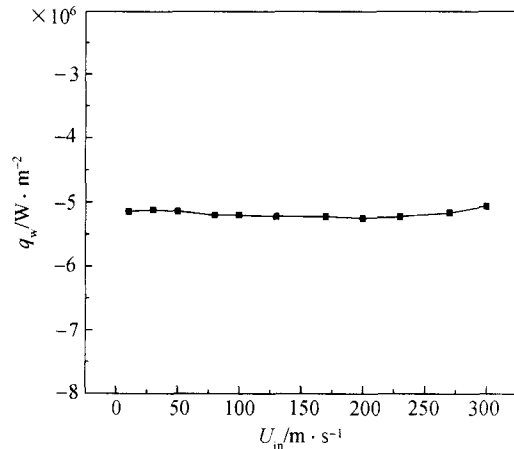


Fig. 8. Variation of the total heat flux with the free stream velocity with $Kn = 1.0$ and $AR = 5$.

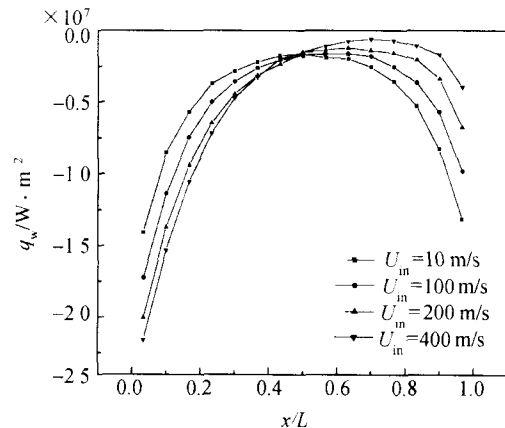


Fig. 9. Variation of the local heat flux with the free stream velocity with $Kn = 1.0$ and $AR = 5$.

3 Conclusion

(1) As far as the heat transfer in microchannel is concerned, the heat flux is mainly located in the inlet and outlet. When AR is small, the heat exchange will happen all over the channel. With the increasing AR , the middle region of the channel in which the heat flux approaches zero become larger and the gas flow is much closer to isothermal flow whose temperature is almost the same as that of the surface. The total heat flux increases with the increasing Kn number and decreases with increasing AR .

(2) The gas temperature slipping happens on the surfaces of the channel, and the higher the

Kn number, the greater the slipping temperature difference.

(3) In subsonic flow, the free stream velocity has no effect on the total heat transfer rate of a microchannel, but it influences the local heat flux distribution along the channel.

Acknowledgments This work was supported by the National Key Project of Fundamental R&D of China (Grant No. G2000026303) and the National Natural Science Foundation of China (Grant No. 50076034).

References

1. Liu, J. . *Micro/Nano-scale Heat Transfer (in Chinese)*, Beijing: Science Press, 2001, 1—6.
2. Chen, X. . *Dynamics and Its Application in Heat Transfer and Fluid Flow (in Chinese)*, Beijing: Tsinghua University Press, 1996, 1—74.
3. Bird, G. A. , *Molecular Gas Dynamics and the Direct Simulation of Gas Flows*, New York: Oxford University Press, 1994.
4. Wu, Q. F. , Chen, W. F. , *DSMC Method in Thermochemistry and Nonequilibrium Flow of Rarefied Gas with High Temperature (in Chinese)*, Changsha: National University of Defence Technology Press, 1999, 61—71.
5. Cheng, C. H. , Liao, F. L. , DSMC analysis of rarefied gas flow over a rectangular cylinder at all Knudsen numbers, *J. Fluids Engineering*, 2000, 122: 720—729.
6. Bird, G. A. , *Molecular Gas Dynamics*, Oxford: Clarendon Press, 1976.
7. Mavriplis, C. , Ahn, J. C. , Goulard, R. , Heat transfer and flow fields in short microchannels using direct simulation Monte Carlo, *J. Thermophysics and Heat Transfer*, 1997, 11(4): 489—496.